

CAD-BASED MODELING FOR 3D PARTICLE TRANSPORT

Yican Wu and Qin Zeng

Institute of Plasma Physics, Chinese Academy of Sciences,
P.O. Box. 1126, Hefei, Anhui, 230031, China
School of Nuclear Science and Technology,
University of Science and Technology of China, Hefei, Anhui, 230027, China
ycwu@ipp.ac.cn; qzeng@ipp.ac.cn

Lei Lu

Institute of Plasma Physics, Chinese Academy of Sciences,
P.O. Box. 1126, Hefei, Anhui, 230031, China
School of Nuclear Science and Technology,
University of Science and Technology of China, Hefei, Anhui, 230027, China
lulei@ipp.ac.cn;

ABSTRACT

Describing and verifying of the models for three-dimensional neutron transport simulation based on Monte Carlo (MC), discrete ordinates (S_N) and MC- S_N coupled methods are time-consuming and error-prone. The conversion algorithm and corresponding CAD-based interface programs have been developed to achieve the bi-directional conversion between commercial CAD systems and the neutron transport simulation codes including MCAM (Monte Carlo Automatic Modeling system) program for MC simulation, SNAM (S_N Automatic Modeling system) program for S_N simulation and RCAM (Radiation Coupled Automatic Modeling System) program for MC- S_N coupled simulation. This paper summarizes the key techniques and main functions of the programs and the application to shielding analysis and neutronics design in CAD-based modeling for 3D complex geometries of the advanced reactor systems. The results and analyses have demonstrated the feasibility, effectiveness and maturity of the three programs for the complex fusion applications.

Key words: neutronics modeling; interface program; CAD-based simulation

1. INTRODUCTION

Particle transport simulations are widely used in fields such as nuclear engineering, neutron welling, radio-therapy and space sciences. Describing and verifying the geometry model manually in text format, however, are the most complex tasks of the simulations codes. To solve the modeling of large and complex geometries, recent advances in modeling tools for radiation transport simulation enable an increased fidelity and accuracy in modeling complex geometries in advanced reactor systems such as fusion and accelerator facilities. Models are routinely generated as part of a computer-aided drafting/design process. Future neutronics calculations will increasingly be based on these 3-D CAD-based geometries, allowing enhanced model complexity and improved quality assurance.

In order to meet challenges of neutronics analyses and design, FDS Team has investigated the

methodology of modeling and visualization of particle transport simulation for years. Making using of this methodology, FDS Team has developed three integrated CAD-based interface programs [1,2] between CAD systems and transport simulation codes for MC simulation (named MCAM - Monte Carlo Automatic Modeling system [3-7]), for S_N simulation (named SNAM - S_N Automatic Modeling system [8,9]) and for MC- S_N coupled simulation (named RCAM - Radiation Coupled Automatic Modeling System) to address the predicaments of transport simulation modeling. The programs make this possible by removing the tedious, time-consuming and error prone process of manually translating these CAD-based geometries into the geometric representations needed as input to these nuclear analysis computational tools.

The programs have been tested with the ITER (International Thermo-nuclear Experimental Reactor) benchmark model [5,6,8] successfully. Up to now they have been applied to fusion neutronics analyses, such as the shielding analyses of ITER [10-15] and the EAST experimental tokamak [16], the neutronics design of the FDS series fusion power plants [17] in China and the compact reversed shear tokamak CREST [18] in Japan and the neutronics analyses of Chinese dual-functional lithium lead (DFLL) test blanket module in ITER [19]. The results and analyses have demonstrated the feasibility, effectiveness and maturity of the three programs for the complex fusion applications.

2. METHODOLOGY

As the chief theories, the methodology of conversion of CAD model to input data of particle transport code i.e. BREP to CSG, of the reversion of input data to CAD model i.e. CGS to BREP, of the healing and checking CAD model, of the spline surface approximating and of the mixed rendering of geometry models and 3D volume data has been introduced in the following.

2.1 Conversion of BREP to CSG

Current CAD modeling systems use a boundary representation (BREP) format to define three-dimensional boundaries of the solid. A BREP model is represented as a collection of geometric elements such as vertices, edges and surfaces together with topological information which limits them. However, many Monte Carlo transport simulation codes use special Constructive Solid Geometry (CSG) representation which can define complex 3D geometry by half-spaces and a serial of Boolean operations on it. Generating the MC model from CAD model in essence is conversion of BREP to CSG. Conversion algorithm based on decomposition is adopted in MCAM, by using of the decomposing surfaces, the CAD model is subdivided into a set of primitive models. The primitive model is defined as model whose surfaces do not include decomposition surface and which can be described by intersection of the half spaces of it. The key step is selection of decomposition surface in the process of conversion. Dominating surface refers to surface or curve which makes the number of primitive models subdivided less. Selection of decomposition surface based on heuristic algorithm and feature recognition can achieve that [20]. However, a primitive model contains curved surface may not be represented solely by half space of boundary surfaces, so additional separating surfaces need to be constructed and added into surfaces list of the primitive model to generate the sufficient boundary set.

Furthermore, the whole problem space needs to be defined by many MC codes. However, CAD model includes only the parts. Void filling function of MCAM is realized by splitting the whole space into many sub-spaces and describing the complementary of many primitive models in sub-spaces.

2.2 Conversion of CSG to BREP

Neutronics model is described in the text file, checking and revising the neutronics model is difficult and time-consuming. Although some methods have been developed all over the world, those methods based on ray tracing to great extent have limits that the models can not be saved and edited. MCAM provides the function of conversion of CSG to BREP aiming at verifying, saving and editing the model. Based on the conversion of CSG to BREP, neutronics model can be visualized from text format, and get three-dimension CAD model. Particle transport simulation codes usually use cell and surface cards define geometry model. In order to achieve conversion of CSG to BREP, the half spaces of surfaces and Boolean operations were parsed from Monte Carlo input file for generating CSG tree. Leaves nodes represent half spaces of surfaces defined in surface card, interior nodes represent Boolean operations (intersection, union, subtraction). By in-order traversal of those binary CSG trees, the CAD model can be generated. Usually, there are two ways of describing cell card: surface-related and component-related. As for surface-related, the leaves nodes refer to half spaces of surfaces, as for the latter, these nodes represent primitive solids such as box, sphere, cylinder, etc.

With the respect to cards of repeated structure like fill card, universe card, the nesting usually takes place. It results in difficulty of traversing CSG trees. Hash table which storing indexes of U card is used to deal with this problem. We used three dimensions geometry kernel based on BREP to implement conversion of CSG to BREP, and saved the CAD model in neutral files, so it can be imported into commercial CAD systems for further checking and editing.

2.3 Model Healing and Checking

Generally, the input CAD models are created in some other CAD modeling system and read into MCAM. Due to imprecise and limitations of CAD data transfer, the problems such as gaps between entities, and the absence of topology connectivity information arise. The healing function is to detect and correct such problems to make the input CAD model available, including tolerant stitching of the inconsistent vertices in solid, tightening gaps of disconnecting edges and surfaces and rebuilding topology relationship of geometry elements.

The checking function has been developed for detecting and removing the gaps and overlaps in input CAD model, which is unallowed in geometry of MC codes. The tolerance of minimum distance is predetermined, so if the distance between two boundary surfaces of adjacent entities is less than the tolerance, the boundary surfaces will be merged so as to eliminate the gaps and overlaps. Besides, the Boolean subtraction operation can be adopted direct to remove the large overlaps between two entities.

2.4 Spline Surface Approximating and Fitting:

Generally, CAD systems employ NURBS (Non-Uniform Rational B-Splines) surfaces to describe the complex shape of CAD models. Besides, some elemental analytic surfaces are included as complement, such as plane, sphere, cylinder, cone and torus. However, geometric representation in MC codes is based on Boolean combination of 1st surface (plane), 2^{ed} surfaces (sphere, cylinder, cone, ellipsoid, hyperboloid, paraboloid) and special 4th surface (torus and elliptical torus). Each surface divides the analysis universe into two pieces.

The elemental analytic surfaces of CAD model can be translated into surface equations of MC code direct; however, the NURBS surfaces descriptions can not be recognized. Therefore, the input CAD model needs large-scale simplification manually.

On the basis of the different surface representations of CAD system and MC code, NURBS surface can be categorized under two types: Free NURBS surfaces that can not be represented by surface equations of MC codes and Special NURBS surfaces that represent general quadric surfaces actually, including ellipsoid, hyperboloid, paraboloid. Approximating and fitting algorithm are developed for processing the two types of NURBS surfaces respectively.

Approximating algorithm is find of a series of simple surface patches can simulate the original complex surface, MCAM adopts adaptive subdividing method to generate the approximating facets (polygons and triangles), the parameters of maximum distance between a facet and the original surface and minimum dimension of facet are predefined to control the approximating degree and the quantity of facets. After approximating, a new BREP model without NURBS surface is reconstructed based on the geometry information of approximating facets.

Fitting algorithm is to translate the ellipsoid, hyperboloid, paraboloid represented as NURBS surfaces in CAD model into general quadric surfaces described in MC codes, whose implicit equation is:

$$f(x, y, z) = C_0 + C_1x^2 + C_2y^2 + C_3z^2 + C_4xy + C_5yz + C_6zx + C_7x + C_8y + C_9z \quad (1)$$

Then the problem of fitting is calculation of the parameters $s = \langle C_0, C_1, \dots, C_9 \rangle^T$ of $Z(f)$, given a finite set of data points $\{p_i, i = 1, \dots, n\}$ on NURBS surface, which is usually cast as minimizing the mean square distance from data points to the surface $Z(f)$ [21].

2.5 Mixed Rendering of Geometry Models and 3D Volume Data

Complex geometry models and volumetric calculation results are involved in particle transport simulation processes, and there are various relationships between geometry models and 3D result data, such as spatial relationships. To grasp these relationships is very important for both geometry model analysis and volumetric result data analysis. But most visualization methods can only display geometry models or volume data, which makes it impossible to represent those relationships. This paper presents a mixed rendering method to resolve the problem.

Mixed Rendering method's basic idea is to take both geometry models and volume data as transparent objects, and render them in the same scene. The key problem of mixed rendering is transparency rendering [22], which is one of the classic difficult problems in computer graphics community. Ray tracing algorithm [23] can accurately imitate ray reflection and refraction, and is a good method for transparency rendering. But it couldn't realize real-time interactive

rendering on common personal computers because of its computational intensity. Most graphics applications adopt triangle sorting based alpha blending technique to implement transparency rendering [24], but the time-consuming triangle sorting and complex triangle splitting is also a problem.

The basic principle of depth peeling technique [25] is to sequentially render a series of images of the scene along an indicated view direction, and to synthesize a result image by blending those series images based on alpha blending technique. Based on depth peeling technique, FDS Team implements transparency rendering on programmable graphic process unit (abbreviated as GPU) by CG programming, thereby realizes mixed rendering of geometry models and 3D volume data with common visualization algorithms.

3. PROGRAMS AND BENCHMARKING

3.1 Programs

Based on the above-mentioned methodology, MCAM, SNAM and RCAM, the three modeling programs, have been developed to support the modeling of particle transport in complicated 3D geometry [1].

MCAM is an integrated interface program between CAD systems and MC codes. Besides the accurate bi-directional conversion between CAD engineering models and neutronics models for MC codes, MCAM also supports model creating, CAD model fixing, model analyzing and editing, which make it an integrated modeling environment for MC particle transport simulation codes. The current version (Version 4.7) of MCAM supports MCNP/MCNPX [26,27] on the mature stage, and the advanced version supporting other MC simulation codes such as EGS[28] and TRIPOLI[29] and even the voxel-based human dosimetry modeling function for the ARTS [30,31] (Accurate Radio Therapy System) has been developed as well.

SNAM is an integrated interface program between CAD systems and S_N codes. It can convert CAD engineering models created in commercial CAD software systems into neutronics models, i.e. the input file for S_N codes. Moreover, the existing input files created for S_N codes can also be automatically parsed and converted back to CAD files by SNAM. SNAM can also visualize the calculating results of S_N codes, which facilitates the user to process the output of S_N codes and easily find the data relationships with the functional module named SVIP. The current version of SNAM supports TORT [32] and VisualBUS [2].

RCAM is designated to support the coupled MC- S_N simulation of complex and large nuclear systems so that the simulation codes could be cooperated to carry out the actual coupled calculations. RCAM combined the functions of MCAM and SNAM to generate the input files simultaneously for MC and S_N codes calculation for a large and complicated system by specifying a coupled transitional zone as schematically. Furthermore, RCAM can achieve bi-directional conversion between MC models and S_N models.

3.2 ITER Benchmarking

The purpose of ITER benchmark exercise was to compare a variety of emerging solutions for the use of CAD geometries in neutron transport calculations. ITER benchmark model, based on a 40 degree toroidal segment of the ITER machine and created in CATIA V5 and exported in STEP format, is issued by ITER IT (International Team) to benchmark the CAD/MCNP programs being developed in the ITER PTs (Participant Teams). The detail introduction of the model has been shown in Reference [1]. The benchmark participants are the FDS Team of the Chinese Academy of Science Institute of Plasma Physics (ASIPP) with the MCAM program, the Karlsruhe Research Center (FZK) with the McCad program [33], the University of Wisconsin (UW) with the DAG-MCNPX direct geometry program [34], the Japan Atomic Energy Agency (JAEA) with the GEOMIT program [35].

The CAD model of ITER benchmark model has been successfully converted into MCNP input file by MCAM [6]. The specified nuclear analyses for the model have been calculated with the widely used transport code MCNP/4C and the data libraries FENDL/2.1[36] including the neutron wall loading (NWL) on the first wall, the neutron flux in divertor cassettes, the nuclear heating in the TF coil inboard legs, and the neutron flux in the mid-plane ports.

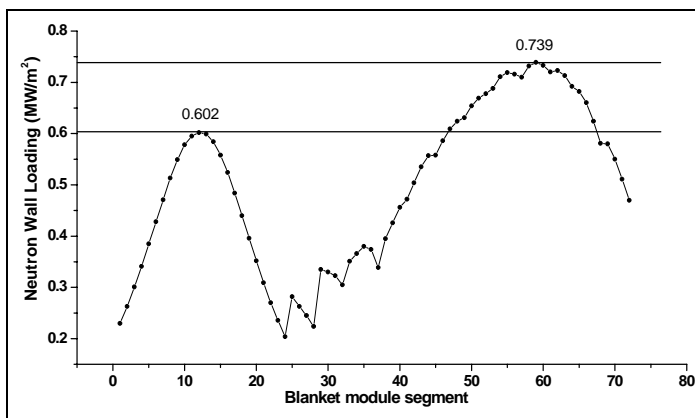


Figure 1. The distribution of neutron wall loading on the first wall

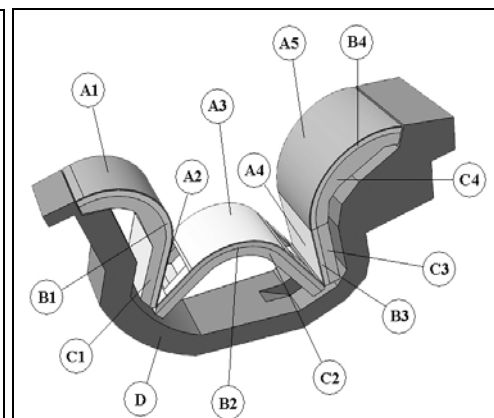


Figure 2. Tally location on divertor cassette loading on the first wall

3.2.1 NWL on the First Wall

The distribution of the NWL on the first wall of the device is a fundamental result. There were 18 blanket modules distributed in the poloidal direction and each blanket module was divided into four equal poloidal segments. The NWL was calculated on the plasma-facing side of these modules and plotted against the length measured from the bottom of the 1st blanket module. Fig.1 shows the distribution of the neutron wall loading on the first wall.

3.2.2 Neutron Flux in Divertor Cassette

The divertor cassette is made of two kind of components with a complex structure that has different purposes: the plasma-facing components for very high heat load removal, called High

Heat Flux Components (HHFCs), and an underlying robust “cassette body”. The primary purpose of this result is to test the ability to model such structures. The neutron flux with four energy groups ($E < 1\text{eV}$, $1\text{eV} < E < 0.1\text{MeV}$, $0.1\text{MeV} < E < 1\text{MeV}$, $1\text{MeV} < E < 20\text{MeV}$) and the total ($E < 20\text{MeV}$) were given on the surface of the divertor cassette and in the structural elements of the cassette. As the surface is the interface between the plasma and the plasma-facing components, it has been segmented to five parts consisted with the components, inner vertical W, inner vertical CFC, dome, outer vertical CFC, outer vertical W. The cassette was signed as A, B, C and D proper to the components, as illustrated in the Fig.2. Table I and Table II give the neutron flux in the energy region from 1MeV to 20MeV and the total region on the surface and in the structural elements. The statistical errors of the results are less than 1%. The maximum surface flux and volume flux in the divertor are $1.33 \times 10^{14} \text{n/cm}^2/\text{s}$ and $1.21 \times 10^{14} \text{n/cm}^2/\text{s}$, respectively, where are both in A1 which is the nearest component around the plasma.

Table I. The neutron flux on the divertor surface ($\text{n/cm}^2/\text{s}$)

Divertor Surface Flux	1MeV <E< 20MeV	Total
Inner Vertical Target W	$4.30 \cdot 10^{13}$	$1.33 \cdot 10^{14}$
Inner Vertical Target CFC	$1.41 \cdot 10^{13}$	$6.89 \cdot 10^{13}$
Dome	$4.12 \cdot 10^{13}$	$1.26 \cdot 10^{14}$
Outer Vertical Target CFC	$1.94 \cdot 10^{13}$	$6.40 \cdot 10^{13}$
Outer Vertical Target W	$4.15 \cdot 10^{13}$	$1.21 \cdot 10^{14}$

Table II. The neutron flux in the divertor cassette ($\text{n/cm}^2/\text{s}$)

Divertor Volume Flux		1MeV <E< 20MeV	Total
A1	Inner Vertical Target W	$3.73 \cdot 10^{13}$	$1.21 \cdot 10^{14}$
A2	Inner Vertical Target CFC	$1.14 \cdot 10^{13}$	$6.22 \cdot 10^{13}$
A3	Dome	$2.93 \cdot 10^{13}$	$9.34 \cdot 10^{13}$
A4	Outer Vertical Target CFC	$1.56 \cdot 10^{13}$	$5.71 \cdot 10^{13}$
A5	Outer Vertical Target W	$3.81 \cdot 10^{13}$	$1.15 \cdot 10^{14}$
B1	PFC cooling structure (Inner Vertical Target)	$1.77 \cdot 10^{13}$	$7.69 \cdot 10^{13}$
B2	PFC cooling structure (Dome)	$1.88 \cdot 10^{13}$	$7.26 \cdot 10^{13}$
B3	PFC cooling structure (Outer Vertical Target CFC)	$7.02 \cdot 10^{12}$	$3.63 \cdot 10^{13}$
B4	PFC cooling structure (Outer Vertical Target W)	$2.54 \cdot 10^{13}$	$9.31 \cdot 10^{13}$
C1	SS part of PFC (Inner Vertical Target)	$6.41 \cdot 10^{12}$	$3.59 \cdot 10^{13}$
C2	SS part of PFC (Dome)	$8.22 \cdot 10^{12}$	$4.08 \cdot 10^{13}$
C3	SS part of PFC (Outer Vertical Target CFC)	$1.66 \cdot 10^{12}$	$1.32 \cdot 10^{13}$
C4	SS part of PFC (Outer Vertical Target W)	$7.95 \cdot 10^{12}$	$3.83 \cdot 10^{13}$
D	Cassette Body	$6.93 \cdot 10^{11}$	$3.46 \cdot 10^{12}$

3.2.3 Nuclear Heating in TF Coil Inboard Legs

The TF magnets are key components that influence the performance of ITER. The protection of the magnets especially their inboard legs against radiation and its influence on the performance of the ITER is one of the critical issues that receive special attention during the courses of the ITER study from the ITER-98 to the current design. The benchmark model includes two TF coil inboard legs. The straight segment of the inboard TF coil ($-395.10 < z < 400.90$ cm) was divided into 10 axial segments. For each segment, the nuclear heating of two inboard legs was presented in Fig.3.

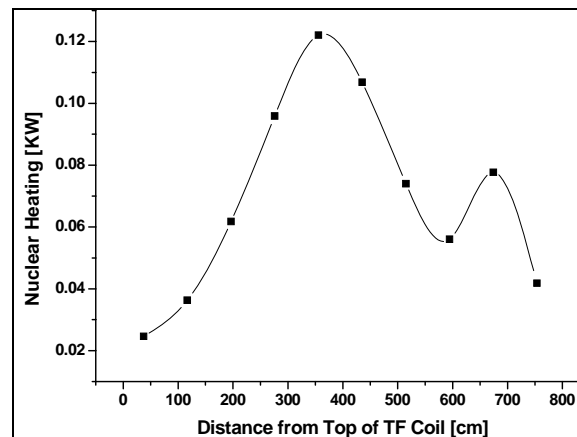


Figure 3. Total TF coil heating in two inboard legs

The total TF nuclear heating of all the 18 inboard legs is 9.03KW. A correction factor of 1.2 was used for the value taking into account an effect of neutron streaming through the inboard blanket flexible joints in the inner vacuum vessel structure. Then a heterogeneity effect of the layered vacuum vessel structure 1.2 was also taken into account to correct energy deposition in the inboard leg segments where the thickness of the vacuum vessel is minimal. The statistical errors of the results are less than 10%. The total nuclear heating in all inboard legs is less than the limited value 10.7KW in ITER nuclear analysis report NAG-201[38].

3.2.4 Neutron Flux in Mid-plane Ports

The radial flux profile across dummy port plug and shield plug was estimated. This was a straightforward calculation involving multiple scattering events and deep penetration which require the use of variance reduction techniques. The results were affected by the geometry configuration and the associated material compositions. The neutron flux has been calculated for radial segments (approximately 5cm thickness) of the upper dummy port plug, averaged over the poloidal height and the toroidal width, as shown in the Fig.4. The same segmentation scheme has been applied for the shield plug behind the dummy port plug. Several small spherical detectors have been placed in the geometry as locations to calculate the neutron flux in the mid-plane ports. These results are intended to test the ability to model the effect of streaming along gaps in the geometry. The radial distance has been reported at the center of the detector spheres from the central axis of the benchmark model.

The neutron flux profile in radial distance was shown Fig.5. The upper test blanket dummy and port plug are homogenized with 30 vol. % of water and 70 vol. % of 316 LN-I (G) steel. The neutron flux of the farthest sphere is 1.36×10^9 n/cm²/s. The statistical errors of the results are less than 10%. These results only are references given the test blanket and the shield plug design because of the dummy material and geometry of test blanket and port plug.

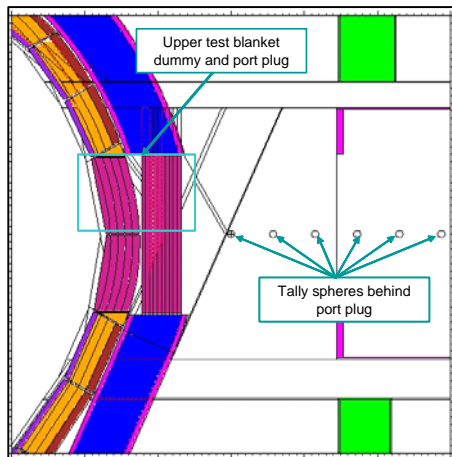


Figure 4. Tally regions in the mid-plane port in radial distance

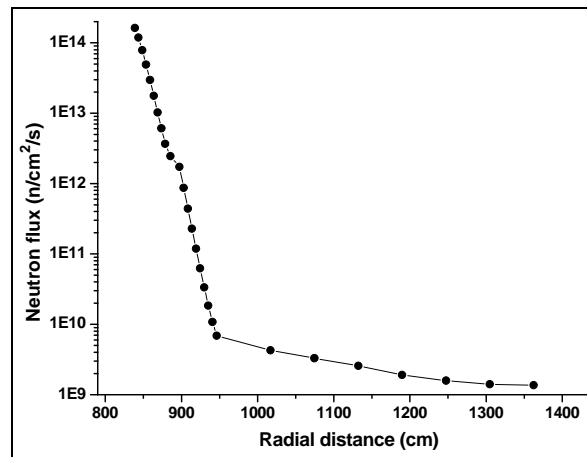


Figure 5. Neutron flux distribution in the mid-plane port

The comparison and analyses of the above results from the four participants were shown in the reference [7]. The CAD interface based method has been proven to be efficient and practicable for MC automatic modeling. As an implementation of this approach, MCAM is capable to convert large complex 3-D CAD models into MCNP input files and vice versa. Besides the conversion functions and basic modeling ability, MCAM is also a fully featured visualization and model analysis tool for MC simulation codes. Now MCAM has passed the ITER benchmark model conversion test and the existing ITER neutron model reversion test. It means that MCAM is an efficient productivity tool in nuclear design and analysis.

3.3 Comparison Testing of the Programs

The main functions of the three programs (MCAM/SNAM/RCAM) have been tested by using the complex geometry of the 3D ITER benchmark model, shown in the reference [1]. The CAD model was converted into the input files of simulation codes automatically with MCAM/SNAM/RCAM, and neutron fluxes in the inboard blanket modules of ITER benchmark model were calculated using MC and S_N codes. The shielding analysis after the bioshield was modeled by RCAM and calculated by coupled MC- S_N transport simulation.

The CAD model was converted into the input files of simulation codes automatically with MCAM and SNAM, and neutron fluxes in the inboard blanket modules of ITER benchmark model were calculated using MC and S_N codes. The MC transport calculation was performed by

using MCNP/4C with the data library FENDL-2.1 and TRIPOLI with the data library ENDF/B-VI, with the statistical errors of the results of less than 3%. The S_N transport calculation was carried out by TORT with the data library MATXS10 (30 neutron groups, 12 gamma groups) [24]. The Legendre expansion of the scattering kernel is P_1 and the angular quadrature set used by TORT is S_4 . The neutron fluxes in the inboard blanket (Module 4) were compared. As shown in Table III, the calculation results by different codes agreed well and the peak difference was 12%. These differences may lie on the different data libraries used, as well as the different simulation methods, which need to be investigated further.

Table III. Neutron Flux in Module 4

Radial range	Neutron flux ($1/\text{cm}^2\cdot\text{sec}$)				
	TORT	MCNP		TRIPOLI	
		Result	Error (%)	Result	Error (%)
359.35 -370	$1.359 \cdot 10^{12}$	$1.550 \cdot 10^{12}$	2.16	$1.493 \cdot 10^{12}$	2.73
370.35 -381.5	$4.841 \cdot 10^{13}$	$4.967 \cdot 10^{12}$	1.12	$4.723 \cdot 10^{12}$	1.45
381.5 -393	$1.940 \cdot 10^{13}$	$1.828 \cdot 10^{13}$	0.61	$1.785 \cdot 10^{13}$	0.74
393 -397.35	$4.486 \cdot 10^{13}$	$4.153 \cdot 10^{13}$	0.50	$4.092 \cdot 10^{13}$	0.63
397.35 -404.5	$7.465 \cdot 10^{13}$	$6.999 \cdot 10^{13}$	0.35	$6.959 \cdot 10^{13}$	0.40

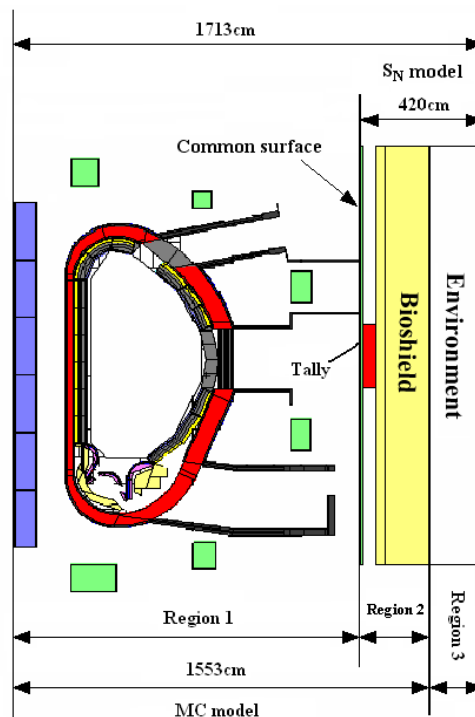


Figure 6. Processing of ITER benchmark model by RCAM

The shielding calculation of ITER based on conversional methods e.g. only MC simulation or S_N simulation is difficult due to the complex geometry and the large dimension, especially including bio-shield of meters thickness. In this benchmark, RCAM is used to generate the input files of MC and S_N codes respectively as schematically shown in Fig.6. The whole model was divided by the common surface (the inner surface of the cryostat) and the outer surface of bioshield into three parts: the source modeling region (Region 1) inside the common surface, transitional region (Region 2) between the common surface and the outer surface of bioshield and the environment region (Region 3). For the purpose of testing RCAM, the neutron flux in the tally area was calculated, respectively, by MCNP with the data library FENDL-2.1 based on the MC model (Region 1+ Region 2) and by the S_N code TORT the data library MATXS10 based on the S_N model (Region 2 +Region 3) with the surface source obtained from the MCNP calculation. The calculated results given in Table IV have shown an acceptable difference ($\sim 13\%$) between the two approaches, which may be caused by different transport methods (MC and S_N methods) and different nuclear data libraries (point-wise and multi-group libraries) etc.

Table IV. Neutron Flux in Tally Area

MCNP		MC - S_N Coupled	Error
Result	Stat. error	1.817 10^8	12.95%
1.609 10^8	6.14%		

4. APPLICATION

The three CAD-based programs have been applied to fusion neutronics analyses, some examples are given in the following:

(1) ITER reference model update and DFLL-TBM neutronics analyses: the ITER neutronics reference model named “BRAND” has been updated on the basis of the latest CAD design and extended from 20 degrees to 40 degrees in the toroidal direction by MCAM[13]. Furthermore, the CAD model of the DFLL-TBM (Dual Functional Lithium Lead Test Blanket Module) design proposed by China was integrated in the equatorial port of the updated model and converted into an MCNP input file by MCAM for detailed neutronics analysis on the tritium breeding ratio and the distribution of nuclear heat in DFLL-TBM [17].

(2) ITER shielding analysis calculation: In the radiation shielding analyses of hot cell building [10], the required thickness for ceiling slab of hot cell was estimated with the 3D model produced by MCAM. The dose rates after shutdown around and in the port limiter equatorial port and the neutron fluxes and U-235 fission rate at the neutron flux box was performed by ITER IT with MCAM [11]. The fast neutron flux, nuclear heat of the super-conducting magnets and the shutdown dose rate around the upper ports were calculated to estimate the shielding capacity of the new upper ports design by using MCAM [12]. The assessment and optimization of the shielding of the electron cyclotron wave launching system in the ITER upper port to ensure the radiation loads to adjacent components such as the vacuum vessel are tolerable were

implemented by A. Serikov and the co- authors in FZK by using MCAM [15].

(3) Nuclear analyses of EAST and conceptual of fusion reactor: the nuclear heating and irradiation field analyses of TF coil in EAST (Experimental Advanced Superconductor Tokamak) were performed by the interface programs [16]. Furthermore, the programs were applied to the neutronics design of the FDS series fusion power plants including the fusion-driven subcritical system (named FDS-I), the fusion electrical generation reactor (named FDS-II), the fusion-based hydrogen production reactor (named FDS-III) and the spherical tokamak-based compact reactor (named FDS-ST) in China [17] and the compact reversed shear tokamak CREST, a conceptual tokamak reactor design with high plasma, high thermal efficiency, competitive cost and water-cooled ferritic steel components in Japan [18].

The series application results of the programs MCAM, SNAM and RCAM showed good consistence and good improvement of computing efficiency of particle transport simulation and further demonstrated the effectiveness and maturity of the three modeling programs at least for fusion application.

5. SUMMARY

The CAD-based modeling methodology investigated by FDS Team has been introduced, which has realized the bi-directional conversion between commercial CAD systems and the neutron transport simulation codes and the visualization of mixed rendering of geometry model and 3D volume data. Based on the developed methodology, three interface programs named MCAM, SNAM, RCAM have been developed whose main functions have been tested by using the complex geometry of the 3D ITER benchmark model and applied to the neutronics analyses of advanced reactor systems with complex geometries to produce results with high fidelity. The results and analyses have demonstrated the feasibility, effectiveness and maturity of the three programs for the complex reactor applications. The three CAD-based interface programs provide bridges between the CAD engineering models and particle transport simulations by taking advantage of new computer technique, which may play even more important roles in the quality assurance of nuclear analysis for complex systems in the future.

ACKNOWLEDGEMENTS

Dr. H. Iida from the Japan Atomic Energy Agency helped to take a mass of calculations and gave a lot of helpful suggestions. The authors like to thank Dr. F. Gianfranco, Dr. U. Fischer, Dr. E. Polunovskiy, Dr. N. Taylor, Dr. M. Loughin, etc., who organized the benchmark exercises and prepared the benchmark model of ITER.

REFERENCES

- [1] Y. Wu, FDS Team, "CAD-based interface programs for fusion neutron transport simulation," *Fusion Engineering and Design*, doi:10.1016/j.fusengdes.2008.12.041, 2009.
- [2] Y. Wu, J. Li, Y. Li, et al. "An integrated multi-functional neutronics calculation and analysis code system: VisualBUS," *Chinese J. Nuclear Science & Engineering*, **Vol.27**, pp.365-373 (2007).

- [3] Yican Wu, X. George Xu, “The Need for Further Development of CAD/MCNP Interface Codes,” invited presentation at the American Nuclear Society Annual Meeting, Boston, USA, June 24-28, 2007.
- [4] Y. Wu, Y. Li, L. Lu, et al. “Research and development of the automatic modeling system for Monte Carlo particle transport simulation,” *Chinese J. Nuclear Science & Engineering*, **Vol.26**, pp.20-27 (2006).
- [5] Y. Li, L. Lu, A. Ding, et al. “Benchmarking of MCAM 4.0 with the ITER 3D model,” *Fusion Engineering and Design*, **Vol.82**, pp.2861–2866 (2007).
- [6] P.P.H. Wilson, R. Feder, U. Fischer, et al. “State-of-the-art 3-D radiation transport methods for fusion energy systems,” *Fusion Engineering and Design*, **Vol.83**, pp.824–833(2008).
- [7] Q. Zeng, L. Lu, A. Ding, et al. “Update of ITER 3D basic neutronics model with MCAM,” *Fusion Engineering and Design*, **Vol.81**, pp.2773-2778 (2006).
- [8] H. Hu, Y. Wu, M. Chen, et al. “Benchmarking of SNAM with the ITER 3D model,” *Fusion Engineering and Design*, **Vol.82**, pp.2867-2871 (2007).
- [9] H. Hu, J. Li, Y. Li, et al. “Study on Key Issues of Automatic Modeling for the S_N -method Based Particle Transport Simulation Codes Program,” *Chinese Journal of Nuclear Physics Review*, **Vol.23**, pp. 134-137 (2006).
- [10] H. Iida, L. Lu, “Required Thickness for the Ceiling Slab of Hot Cell Repair Room from Radiation Shielding Point of View,” ITER international analysis report, ID: NAG-259.
- [11] H. Iida, L. Lu, Y. Wu, “Nuclear Analysis of the Port Limiter and Neutron Flux Monitor in the Equatorial Port, An example of MCAM application to ITER design calculation,” ITER international analysis report, ID: NAG-264.
- [12] S. Zheng, Y. Wu, “Nuclear analysis of the Upper Port-Dose rate analysis of the upper port to confirm sufficiency of shielding capacity of final port geometry,” ITER international analysis report, ID: ITA 73-01.
- [13] Q. Zeng, Y. Meng, S. Zheng, Y. Wu, “Update of the ITER 3-D model for MCNP and the Nuclear Data Library for Dose Calculation,” ITER international analysis report, ID: ITA 73-03.
- [14] L. Lu, Q. Zeng, Y. Li, S. Zheng, Y. Wu, “Testing and Application of MCAM for ITER Benchmark model,” ITER international analysis report, ID: ITA 73-08.
- [15] A. Serikov, U. Fischer, Y. Chen, et al. “Neutronics analysis of the ECW launching system in the ITER upper port,” *Fusion Engineering and Design*, **Vol.74**, pp.229-235 (2005).
- [16] J. Zou, Z. He, P. Long, et al. “Modeling of EAST Tokamak for Nuclear Heating Analysis of TF Coil Using SNAM,” *Chinese J. Nuclear Science & Engineering*, to be published in **Vol.29**, 2009.
- [17] Y. Wu, FDS Team, “Conceptual design activities of FDS series fusion power plants in China,” *Fusion Engineering and Design*, **Vol.81**, pp.2713-2718 (2006).
- [18] Q. Huang, S. Zheng, L. Lu, et al. “Neutronics Analysis for A Compact Reversed Shear Tokamak CREST,” *Fusion Engineering and Design*, **Vol.81**, pp.1239-1244 (2006).
- [19] Y. Wu, FDS team. “Design analysis of the Chinese dual-functional lithium lead (DFLL) test blanket module in ITER,” *Fusion Engineering and Design*, **Vol.82**, pp.1893–1903 (2007).
- [20] Luo Yue-tong, Research on Algorithm of Auto-adding Aided surface in MCNP modeling, *Journal Of System Simulation*, **vol.14**, pp.470-473(2002).
- [21] G. Taubin, “Estimation of planar curves, surfaces and nonplanar space curves defined by implicit equations with applications to edge and range image segmentation,” *IEEE Transaction Pattern Analysis and Machine Intelligence*, **Vol.13**, pp.1115-1138 (1991).

- [22] Jianbing Huang, Michael B. Carter, "Interactive transparency rendering for large CAD models," *IEEE Transactions on Visualization and Computer Graphics*, **Vol.11**, pp.584-595 (2005).
- [23] Kay, Douglas Scott, "Transparency, refraction and ray tracing for computer synthesized images." Master's thesis, Cornell University, Ithaca, N.Y. (January 1979).
- [24] Douglas Scott Kay, Donald Greenberg, "Transparency for computer synthesized images." In Proceedings of the 6th Annual Conference on Computer Graphics and Interactive Techniques, Chicago, Illinois, United States, ACM Press, pp.158-164 (1979).
- [25] A. Mammen, "Transparency and antialiasing algorithms implemented with the virtual pixel maps technique," *IEEE Computer Graphics and Applications*, **Vol.9**, pp.43-55 (1989).
- [26] J.F. Briesmeister (ed.), "MCNP – A General Monte Carlo N-Particle Transport Code, Version 4C," Los Alamos National Laboratory, Report LA-13709-M, April 2000.
- [27] J.S. Hendricks, G.W. McKinney, L.S. Waters, et al. "MCNPX, Version 2.5.E", Los Alamos National Laboratory, Report LAUR-04-0569, February 2004.
- [28] <http://www.irs.inms.nrc.ca/EGSnrc/EGSnrc.html>
- [29] J.P. Both, H. Derriennic, B. Morillon, et al. "A Survey of TRIPOLI-4," proceedings of the 8th International Conference on Radiation Shielding, Arlington, TX USA, April 24-28, pp. 373-380 (1994).
- [30] Y. Wu, G. Li, S. Tao, et al. "Research and Development of an Accurate/Advanced Radiation Therapy System (ARTS)," *Chinese Journal of Medical Physics*, **Vol.22**, pp. 683-702 (2005).
- [31] Y. Wu, G. Song, R. Cao, et al. "Development of Accurate/Advanced Radiotherapy Treatment Planning and Quality Assurance System (ARTS)," *Chinese Physics C (HEP & NP)*, **Vol.32 (Suppl. II)**, pp.1-6 (2008).
- [32] Y.Y. Azmy, F.X. Gallmeier, D.A. Lillie, "TORT Solution for the 3D Radiation Transport Benchmarks for Simple Geometries with Void Region," *Progress in Nuclear Energy*, **Vol.39**, pp.155-166 (2001).
- [33] H. Tsige-Tamirat, U. Fischer, "CAD interface for Monte Carlo particle transport codes, in: The Monte Carlo Method: Versatility Unbounded in a Dynamic Computing World." Proceedings of the Conference, Chattanooga, TN., April 17 - 21, La Grange Park, ANS, 2005.
- [34] M. Wang, T. Tautges, D. Henderson, et al. "Three-dimensional modeling of complex fusion devices using CAD-MCNPX interface," *Fusion Science and Technology*, **Vol.47**, pp.1079-1083 (2005).
- [35] S. Sato, H. Iida, T. Nishitani, "Development of a CAD/MCNP interface program prototype for fusion reactor nuclear analysis," *Fusion Engineering and Design*, **Vol.81**, pp.2767-2772 (2006).
- [36] The IAEA Nuclear Data Section, "FENDL-2.1 Fusion Evaluated Nuclear Data Library, Vienna," Austria, INDC (NDS)-467, Version December 2004.
- [37] H. Iida, V. Khripunov, L. Petrizzi, "Nuclear Analysis Report," ITER Garching Joint Work Site, June 2001. ID: NAG-201-01-06-17-FDR.